

ORIGINAL RESEARCH

# Interleukin-29 Accelerates Vascular Calcification via JAK2/STAT3/BMP2 Signaling

Nannan Hao , MD\*; Zihao Zhou , MD\*; Feifei Zhang, MD\*; Yong Li, MD; Rui Hu, MD; Junjie Zou, MD; Rui Zheng, MD; Lei Wang, MD; Lingxiao Xu, MD; Wenfeng Tan, MD; Chunjian Li , MD; Fang Wang , PhD

**BACKGROUND:** Vascular calcification (VC), associated with enhanced cardiovascular morbidity and mortality, is characterized by the osteogenic transdifferentiation of vascular smooth muscle cells. Inflammation promotes VC initiation and progression. Interleukin (IL)-29, a newly discovered member of type III interferon, has recently been implicated in the pathogenesis of autoimmune diseases. Here we evaluated the role of IL-29 in the VC process and underlying inflammatory mechanisms.

**METHODS AND RESULTS:** The mRNA expression of IL-29 was significantly increased and positively associated with an increase in BMP2 (bone morphogenetic protein 2) mRNA level in calcified carotid arteries from patients with coronary artery disease or chronic kidney disease. IL-29 and BMP2 proteins are colocalized in human calcified arteries. IL-29 binding to its specific receptor IL-28R $\alpha$  (IL-28 receptor  $\alpha$ ) (IL-29/IL-28R $\alpha$ ) inhibited the proliferation of rat vascular smooth muscle cells without altering cell apoptosis or migration. IL-29 promoted the calcification of rat vascular smooth muscle cells and their osteogenic transdifferentiation in vitro as well as the rat aortic ring calcification ex vivo, induced by the calcification medium or osteogenic medium. The procalcification effect of IL-29 was reduced by pharmacological inhibition of IL-29/IL-28R $\alpha$  binding as well as suppression of janus kinase 2/signal transducer and activator of transcription pathway activation, accompanied by decreased BMP2 expression in the cultured rat vascular smooth muscle cells.

**CONCLUSIONS:** These results suggest an important role of IL-29 in VC development, at least partly, via activating the janus kinase 2/signal transducer and activator of transcription 3 signaling. Inhibition of IL-29 or its specific receptor, IL-28R $\alpha$ , may provide a novel strategy to reduce VC in patients with vascular diseases.

**Key Words:** interleukin-29 ■ JAK/STAT pathway ■ vascular calcification ■ vascular smooth muscle cell

See Editorial by Cai et al.

Vascular calcification (VC) is characterized by the deposition of calcium phosphate complexes in the arterial wall, and categorized by the intimal and medial calcification, depending on the sites of mineral deposition within the affected vessels.<sup>1</sup> Although it is regarded as a part of the normal aging process, VC has been implicated in the vascular pathogenesis associated with diabetes,<sup>2</sup> atherosclerosis,<sup>3</sup> and chronic kidney disease (CKD).<sup>4,5</sup>

VC is considered as a hallmark of atherosclerosis and a key prognostic indicator of CKD that highly correlates with increased cardiovascular morbidity and mortality.<sup>6</sup>

Although originally thought to be a passive, inevitable, and unregulated pathology process, VC is now appreciated to be an active and cell-mediated process,<sup>7</sup> principally driven by vascular smooth muscle cells (VSMCs)<sup>8</sup> and tightly regulated by an array of inducers

Correspondence to: Fang Wang, PhD and Chunjian Li, MD, Department of Cardiology, The First Affiliated Hospital of Nanjing Medical University, Nanjing 210029, China. Email: wangfangheart@njmu.edu.cn; lijay@njmu.edu.cn

Supplemental Material is available at <https://www.ahajournals.org/doi/suppl/10.1161/JAHA.122.027222>

\*N. Hao, Z. Zhou and F. Zhang have contributed equally.

For Sources of Funding and Disclosures, see page 16.

© 2022 The Authors. Published on behalf of the American Heart Association, Inc., by Wiley. This is an open access article under the terms of the [Creative Commons Attribution-NonCommercial-NoDerivs](#) License, which permits use and distribution in any medium, provided the original work is properly cited, the use is non-commercial and no modifications or adaptations are made.

JAHA is available at: [www.ahajournals.org/journal/jaha](http://www.ahajournals.org/journal/jaha)

## CLINICAL PERSPECTIVE

### What Is New?

- Interleukin (IL)-29 expression is increased in calcified carotid arteries from patients with coronary artery disease or chronic kidney disease, positively associated with BMP2 (bone morphogenetic protein 2) mRNA, and colocalizes with BMP2 protein.
- IL-29, as a proinflammatory cytokine, binds to its specific receptor, IL-28R $\alpha$  (interleukin receptor  $\alpha$ ), on vascular smooth muscle cells, at least partly activating janus kinase 2/signal transducer and activator of transcription 3 signaling pathway to upregulate BMP2 expression in vascular smooth muscle cells, and promotes their osteogenic transformation and calcification.

### What Are the Clinical Implications?

- Our results indicate that inhibition of IL-29/IL-28R $\alpha$  and/or janus kinase 2/signal transducer and activator of transcription 3 signaling using synthetic, small molecule inhibitors may be a useful strategy to reduce vascular calcification-related diseases.

## Nonstandard Abbreviations and Acronyms

<b>ARS</b>	alizarin red S
<b>BMP2</b>	bone morphogenetic protein 2
<b>VC</b>	vascular calcification
<b>VSMC</b>	vascular smooth muscle cell

and inhibitors.<sup>9,10</sup> There is accumulating evidence suggesting that VSMC calcification plays a central role in the development and progression of VC. Importantly, phenotype switching of VSMCs into osteoblasts is considered to be the most critical pathophysiological hallmark of VSMC calcification.<sup>8,11,12</sup> Although the drivers of VSMC phenotypic conversion are distinct in various conditions, the phenotype switching shares some common features: the loss of VSMC markers  $\alpha$ -SMA ( $\alpha$ -smooth muscle actin) and SM22 $\alpha$  (smooth muscle protein 22 $\alpha$ ) and the gain of osteochondrogenic markers including RUNX2 (Runt-related transcription factor 2), BMP2 (bone morphogenetic protein 2), OPN (osteopontin), osteocalcin, ALP (alkaline phosphatase), and Sox9 (sex determining region Y-box 9). Therefore, understanding the regulatory mechanisms of VSMC phenotype switching is crucial for developing new treatments for VC-related diseases. Recent experimental findings suggest that a variety of molecular mechanisms are involved in its regulation, including microRNAs,<sup>13</sup> senescence,<sup>14</sup> endoplasmic reticulum

stress,<sup>15</sup> inflammasome,<sup>16</sup> and autophagy.<sup>17</sup> The regulatory mechanisms of VC have begun a new research focus among vascular biologists and clinicians.

The results from in vitro studies have collectively demonstrated that the proinflammatory cytokines, including interleukin (IL)-1 $\beta$ , IL-6, IL-8, and tumor necrosis factor- $\alpha$  and transforming growth factor- $\beta$ , induce osteogenic differentiation and calcification of VSMCs.<sup>7,18–20</sup> Furthermore, advanced in vivo molecular imaging techniques have demonstrated that inflammation precedes calcification in the initiation phase of VC, and the early activation of proinflammatory pathways induces the osteogenic transformation of VSMCs.<sup>19</sup> Additionally, ex vivo fluorescence reflectance imaging elegantly visualized the real-time association of inflammation and early calcification.<sup>21</sup> Although these findings strongly suggest that systemic and local inflammation initiates the osteogenic activity of VSMCs leading to VC, the key inflammation factors and the mechanisms underlying the VC process remains largely unknown. In-depth studies of the mechanisms in VSMC osteogenic transformation at the initial phase and the identification of key targets for early intervention are critically needed for VC prevention and treatment.

IL-29 is a newly discovered cytokine belonging to the type III interferon (IFN) family (also referred to as IFN- $\lambda$ s), which consists of 3 to 4 members: IFN- $\lambda$ 1 (IL-29), IFN- $\lambda$ 2 (IL-28a), IFN- $\lambda$ 3 (IL-28B), and/or IL- $\lambda$ 4 in humans.<sup>22,23</sup> Because of their functional similarity with type I IFNs, these novel cytokines are considered as interferon-like cytokines. Notably, IL-29 serves as one of the most effective and plentiful types of IFN III in humans. The specific activity of IL-29 is determined, in part, by the location of its receptor subunit IL-28 receptor  $\alpha$  (IL-28R $\alpha$ , also known as IFNLR1) chain, which is expressed on a limited range of cell types (eg, epithelial cells, dendritic cells, neutrophils, synovial fibroblasts),<sup>24,25</sup> and the other common subunit, IL-10 receptor 2 (IL-10R2), is also the chain of the receptor of IL-10, IL-22, and IL-26.<sup>26,27</sup>

Apart from the antiviral activity, recent evidence has indicated the important role of IL-29 in immunomodulation,<sup>24</sup> like other IFNs, via activation of downstream signaling pathways to induce the generation of inflammatory components. As a cytokine, the proinflammatory effect of IL-29 has been extensively documented in some inflammatory disorders, for instance, rheumatoid arthritis<sup>28</sup> and systemic lupus erythematosus.<sup>29,30</sup> Moreover, new evidence has shown that IL-29 exerts a vital effect on inflammatory osteolysis by suppressing bone resorption or modulating the inflammatory microenvironment.<sup>31,32,33</sup> Importantly, the link between osteoporosis and VC in some diseases has been evidenced by sharing common cytokines.<sup>8</sup> As for the interferon cytokine IL-29, its efficient immunoregulatory and inflammatory effect in bone homeostasis suggests

that IL-29 would play an important role in VC. However, there are no reports about the effect and mechanism of IL-29 on VC. Therefore, in this study we sought to investigate the aberrant expression of IL-29 in VC-related disease and explore the mechanism of IL-29 in regulating VSMC phenotypic switching. We found that IL-29 accelerated the VSMC osteogenic transformation and calcification under the calcification medium (CaP) condition via activating the janus kinase 2 (JAK2)/signal transducer and activator of transcription 3 (STAT3) signaling. These findings provide new mechanistic insights into the preventive and therapeutic strategies for vascular diseases.

## METHODS

The data that support the findings of this study are available from the corresponding author on reasonable request.

### Ethics Statement

The study was approved by the ethics committee of the First Affiliated Hospital of Nanjing Medical University. We obtained written informed consent from all patients.

All the animal experimental protocols were approved by the animal ethics and welfare committee of the Nanjing Medical University (Nanjing, China).

### Materials

PrimeScriptRT Master Mix was obtained from TakaRa (Dalian, China) and SYBR Green Polymerase Chain Reaction Master Mix was obtained from Applied Biosystems (Carlsbad, CA). The Annexin V/PI Apoptosis Detection Kit was obtained from Vazyme Biotech (Nanjing, China). Alizarin red S (ARS) staining solution was obtained from Beyotime (Shanghai, China). Vitamin D<sub>3</sub>, dexamethasone, ascorbic acid, and  $\beta$ -glycerophosphate were obtained from Sigma (Saint Louis, MO), and JAK2 antagonist (fedratinib) and STAT3 antagonist (niclosamide) were obtained from Selleckchem (Houston, TX). DMEM and the other culture reagents were from GIBCO (Carlsbad, CA). All antibodies are listed in [Table S1](#).

### Patients and Samples

Carotid artery tissues were obtained from 6 patients without carotid calcification (aged 65.63 $\pm$ 10.90 years), and 7 patients with coronary artery disease (CAD) (aged 65.8 $\pm$ 5.89 years) and 7 patients with chronic kidney disease (CKD) (aged 66.7 $\pm$ 10.88 years) with carotid calcification. All patients underwent carotid artery multidetector computed tomography angiography detection and carotid endarterectomy surgery. The

carotid specimens were collected immediately after carotid endarterectomy, photographed, and macroscopically evaluated based on their visual and morphological characteristics. This study was approved by the ethics committee of the First Affiliated Hospital of Nanjing Medical University.

### Isolation and Culture of Primary Rat VSMCs

Primary rat aortic smooth muscle cells (RVSMCs) were isolated from adult male Sprague Dawley rats (Jiangsu Laboratory Animal Center, Nanjing, China). Briefly, thoracic aortas were cut into 1- to 2-mm sections and cultured in DMEM/F12 medium supplemented with 20% FBS, 100 U/mL penicillin, and 100  $\mu$ g/mL streptomycin at 37 °C in a humidified, 5% CO<sub>2</sub> incubator. After 5 to 7 days, the tissue sections were removed until cells sprouted from them. Migrated VSMCs were digested with 0.25% trypsin, and 3 to 8 passages were used for in vitro experiments.

### Culture of Primary Human VSMCs

Primary human aortic smooth muscle cells were commercially obtained from ATCC (Manassas, VA). Cells were cultured in DMEM medium containing 10% FBS, 100 U/mL penicillin, and 100  $\mu$ g/mL streptomycin (growing medium) at 37 °C in a humidified, 5% CO<sub>2</sub> atmosphere. Cells were used in in vitro experiments up to passage 10.

### Calcification of Cultured VSMCs and Treatments

RVSMCs or human aortic smooth muscle cells were seeded onto a 6-, 12-, or 24- well plates. After 24 to 48 hours, the growing medium was replaced with the CaP medium including DMEM medium, 5% FBS, 100 U/mL penicillin, 100  $\mu$ g/mL streptomycin, 1.5 mM calcium, and 2.0 mM phosphate for a further 2 to 3 days incubation to induce the calcification of VSMCs.<sup>34</sup> In the other calcification model, the osteogenic calcification medium (OGM) consisted of high glucose DMEM medium, 10% FBS, 100 U/mL penicillin, 100  $\mu$ g/mL streptomycin, 0.1  $\mu$ mol/L dexamethasone, 50  $\mu$ g/mL ascorbic acid, 5 mmol/L  $\beta$ -glycerophosphate, 4 mmol/L CaCl<sub>2</sub>, and 1  $\mu$ mol/L insulin. The medium was changed every 3 days for 14 to 17 days to induce calcium deposition in the RVSMCs.

For IL-29 treatment experiments, RVSMCs were seeded onto 6- or 12-well plates for 48 to 72 hours in the growing medium, and then cells were treated with human recombinant IL-29 (1, 10, or 100 ng/mL) in the CaP or OGM medium. DMEM medium with 5% FBS, 100 U/mL penicillin, and 100  $\mu$ g/mL streptomycin was a normal control.

For antagonist experiments, the calcification of RVSMCs was induced as mentioned above, and cells were treated with IL-29 (100 ng/mL) with or without the presence of IL-29 blocking antibodies (1 and 10  $\mu$ g/mL), IL-28R $\alpha$  blocking antibodies (0.1, 1, or 10  $\mu$ g/mL), JAK2 antagonist (fedratinib, 1  $\mu$ M), or STAT3 antagonist (niclosamide, 10  $\mu$ g/mL) in different experiment settings.

After various treatments, cells were collected at different times for further calcification assay, real-time polymerase chain reaction, and Western blot as indicated below.

### Real-Time Cellular Analysis

RVSMC proliferation was examined with real-time cellular analysis using an xCELLigence system according to the manufacturer's instruction (ACEA Biosciences). Briefly, RVSMCs were seeded into an E-plate at a density of 2000 cells per well and incubated in the growing medium at 37 °C in a 5% CO<sub>2</sub> atmosphere. After 24 hours, growing medium containing different concentrations of IL-29 (1, 10, or 100 ng/mL) was added for further incubation over 96 hours. The cell index was exported with real-time cellular analysis software 2.0 (ACEA Biosciences) and was normalized to the value recorded at time point 0 (baseline).

### VSMC Apoptosis Assay by Flow Cytometry

RVSMCs apoptosis was performed after 48 hours treatment with IL-29 (1, 10, or 100 ng/mL) in a 6-well plate, and the cells were harvested and stained according to the manufacturer's instruction using an Annexin V-fluorescein isothiocyanate/propidium iodide staining kit (Vazyme Biotech, Nanjing, China). In brief, after washing twice with cold PBS, cells were suspended in 100  $\mu$ L Annexin V binding buffer and incubated with 5  $\mu$ L Annexin V-fluorescein isothiocyanate and 10  $\mu$ L propidium iodide staining solution for 15 minutes at room temperature away from light. Finally, 400  $\mu$ L Annexin V binding buffer was added to each tube, and the apoptotic rate of the cells was determined by flow cytometry (Beckman CytoFLEX FCM). All data were exported as Flow Cytometry Standard 3.0 documents and analyzed with FlowJo VX10 software.

### VSMC Transwell Assay

Migration assay was performed in a 24-well culture plate by inserting the transwell chamber covered with matrigel basement membrane matrix (pore size, 8.0  $\mu$ m; BD Biosciences) similar to our previous study.<sup>31</sup> RVSMCs ( $1 \times 10^4$  cells per well) suspended in 200  $\mu$ L of the growing medium with 1% FBS were placed in the upper chamber, and 600  $\mu$ L of growing medium containing 1% FBS and IL-29 (1, 10, or 100 ng/mL) were placed in the lower

chamber. Following 24 hours of culture, the noninvasive cells in the upper chamber were removed using a cotton swab, and cells migrated through the membrane were fixed with 4% paraformaldehyde for 30 minutes, and then stained with 0.1% crystal violet for 5 minutes. Invasion cells were determined by counting stained cells in 5 fields per chamber under a light microscope (Zeiss, Germany).

### Vitamin D<sub>3</sub>-Induced Vascular Calcification in Mice

Male C57BL/6 mice (8 weeks old) were purchased from GemPharmatech (Nanjing, China). The animal experiment was approved by the animal ethics and welfare committee of the Nanjing Medical University (Nanjing, China). Mice ( $n=10$ ) were intraperitoneally injected with vitamin D<sub>3</sub> (400 000 IU/kg per day; Sigma) dissolved in olive oil for 14 consecutive days, and the same volume olive oil injection was used as a control.<sup>34</sup> The body weight of mice was recorded every 3 days during the experiment period. At day 28, mice aortas were removed and kept in 4% paraformaldehyde solution for further analysis.

### Rat Aortic Ring Calcification Induction Ex Vivo

Aortas from male Sprague Dawley rats (180–200 g body weight; Jiangsu Laboratory Animal Center, Nanjing, China) were cut into ~5-mm rings and cultured in growing medium. After 24 hours, the growing medium was replaced with the CaP medium as used in vitro above in the absence or presence of IL-29 (100 ng/mL). Aortic segments were further kept at 37 °C in a 5% CO<sub>2</sub> incubator for 6 days, changing the CaP medium every 2 days. On completion of the culture, aortic segments were washed with PBS solution and mounted in optimal cutting temperature compound for further analysis.

### ARS Staining for Calcification Determination

Human aortic smooth muscle cells or RVSMCs were cultured in the CaP medium for 3 days, and the calcification of VSMCs was determined by 0.2% ARS staining (Beyotime, Shanghai, China).

Aortic roots from vitamin D<sub>3</sub>-induced calcified mice and rat aortic rings after ex vivo calcification induction were cut into 5- $\mu$ m frozen sections followed by ARS staining, respectively.

The detailed methods for ARS and optical density quantitation are described in Data S1.

### VSMC Calcium Quantitation

Quantification of the calcification of VSMCs was measured using a QuantiChrom calcium assay kit (BioAssay

Systems). RVSMCs or human aortic smooth muscle cells in a 12-well plate were treated with IL-29 for 3 days under the CaP medium and then decalcified with 0.6M HCl for 24 hours at 4 °C. The supernatants were centrifuged for the calcium content assay according to the kit manufacturer, and the absorbance was measured at a wavelength of 612 nm using a multiplate reader (BioTek Synergy 2). In addition, the cells were solubilized in 0.1 M NaOH and 0.1% SDS, and their protein concentrations were determined using a bicinchoninic acid protein assay kit (Beyotime, Shanghai, China). Finally, the calcium contents were normalized to total protein concentrations.

### Quantitative Real-Time Polymerase Chain Reaction Assay

Total RNA was isolated from VSMCs or arteries using a TRIzol reagent, and reverse transcribed into cDNA using PrimeScript RT Master Mix according to the manufacturer's instructions (Takara, Dalian, China). Quantitative real-time polymerase chain reaction was performed on an Applied Biosystems 7900HT instrument as described previously.<sup>35</sup> Primer sequences are shown in Table S2. All samples were assayed in triplicate, and relative gene expression was determined by the  $2^{-\Delta\Delta Ct}$  method using glyceraldehyde-3-phosphate dehydrogenase as the internal reference.

### Western Blot Analysis

RVSMC were collected after different treatments at an indicated time and lysed with cold lysis buffer supplemented with complete protease and phosphatase inhibitor cocktail to extract proteins. Equal amounts of proteins were loaded for SDS-PAGE, as previously described,<sup>31</sup> and immunoblotting was performed using the specific primary antibodies BMP2, RUNX2, JAK2/phospho-JAK2, signal transducer and activator of transcription 1/2/3/4/5/6, phospho-STAT1/2/3/4/5/6, p38/phospho-p38, ERK/phospho-ERK, JNK/phospho-JNK, glyceraldehyde-3-phosphate dehydrogenase, and the secondary horseradish peroxidase-conjugated antibody. The signals were visualized with enhanced chemiluminescence detection reagent, and protein bands were semi-quantified with the Gel-Pro Analyzer software (Bio-Rad).

### Immunohistochemistry and Immunofluorescence

Human carotid artery tissues (6 calcified and 3 noncalcified samples) were embedded in paraffin. Sections (5  $\mu$ m) were deparaffinized, rehydrated, and then subjected to heat antigen retrieval in 0.01-mM sodium citrate buffer (pH 6.0) and inactivation of endogenous peroxidase with 3% H<sub>2</sub>O<sub>2</sub>. After blocking with 5% BSA, sections were incubated with primary antibodies overnight at 4 °C. After washing, sections were next

incubated with a secondary antibody for 1 hour at room temperature. Finally, the reactions were developed using a 3,3'-N-diaminobenzidine tetrahydrochloride substrate kit. The slides were scanned at  $\times 20$  via an Aperio ScanScope XT slide scanner (Leica Biosystems, Nussloch, Germany), and the digital image was observed with ImageScope software (Leica Biosystems).

For immunofluorescence staining, mice aorta (5  $\mu$ m of frozen sections) or VSMCs were fixed, blocked, and incubated with primary antibodies  $\alpha$ -SMA, IL-28R $\alpha$ , or IL-10R2 at 4 °C overnight respectively, followed by further incubation with a secondary antibody for 2 hours in room temperature. After 4',6-diamidino-2-phenylindole staining (1:5000 dilution) and washing, the slides were mounted, and images were taken with a fluorescence microscope (Zeiss).

### Statistical Analysis

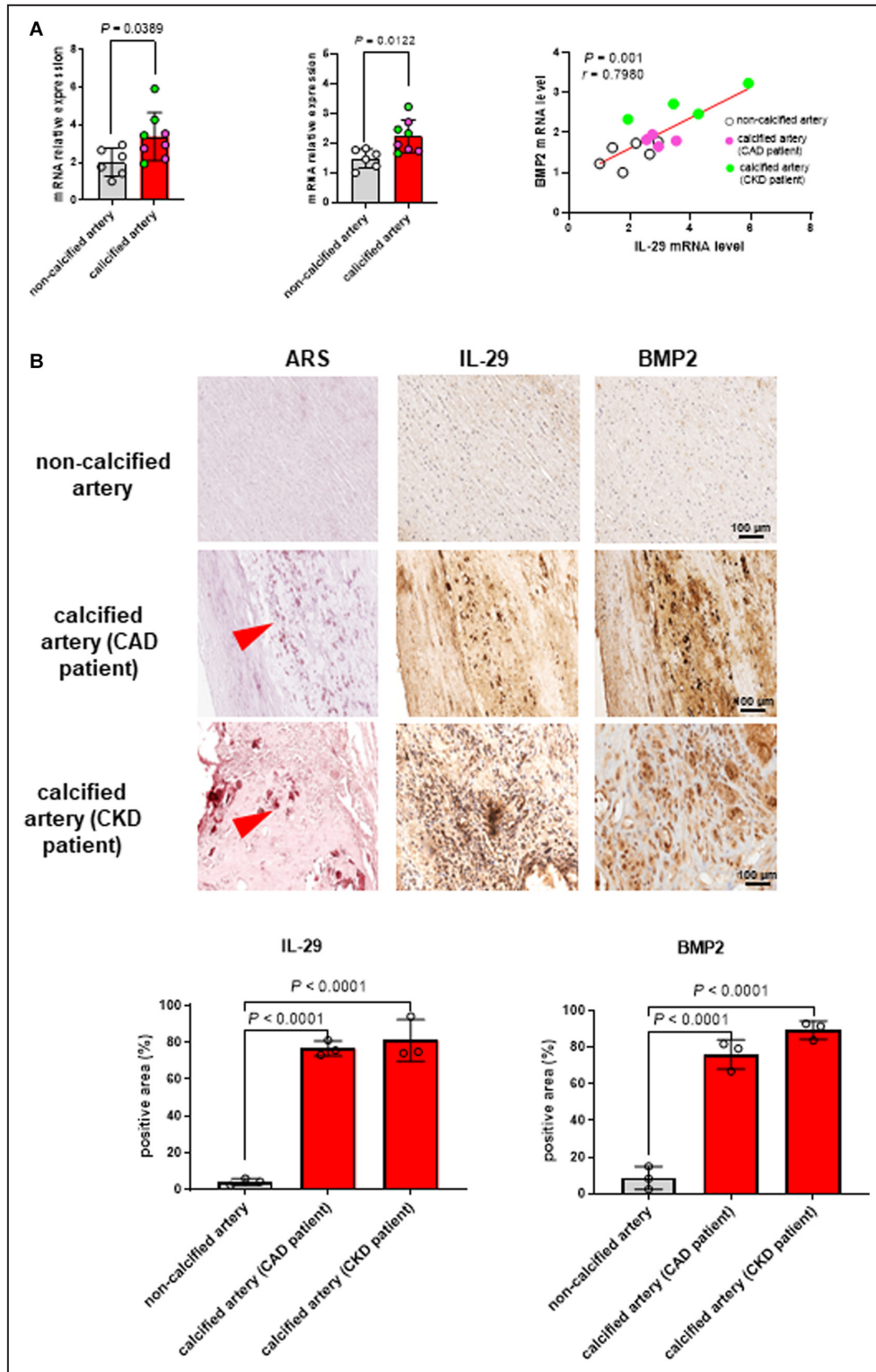
Data were expressed as mean $\pm$ SD or mean $\pm$ SEM. The normality and homogeneity of variance of the data were tested. Differences between the 2 groups were compared by a 2-tailed unpaired Student *t* test or Mann-Whitney *U* test. Multiple-sample comparisons were analyzed by ordinary 1-way ANOVA with Tukey multiple comparisons test or Brown-Forsythe ANOVA followed by Dunnett T3 multiple comparisons test. For correlation analysis, a Pearson correlation test was performed. All statistical analyses and figures were performed using GraphPad Prism 9.0 software (GraphPad Software). *P*<0.05 was considered statistically significant.

## RESULTS

### IL-29 Is Upregulated in the Calcified Arteries of Humans and Mice

To explore whether IL-29 was involved in VC, we first examined the IL-29 expression in the human calcified carotid arteries from patients with CAD and CKD. mRNA expression of IL-29 and BMP2 were significantly higher in the calcified arteries than in the noncalcified control patients (Figure 1A). More importantly, in both groups, IL-29 mRNA expression in the human carotid arteries positively correlated with the BMP2 mRNA expression (Pearson *r*, 0.798; *P*=0.001). Increased RUNX2 (osteogenic gene) and decreased SM22 $\alpha$  (VSMC phenotype gene) mRNA levels were also detected in the human calcified arteries (Figure S1). Additionally, as shown by histological analysis, IL-29 protein levels significantly increased in the calcified carotid arteries from the patients with CAD and CKD in the calcified lesions evidenced by ARS. Furthermore, IL-29 and BMP2 proteins were colocalized in the calcified arterial lesions (Figure 1B).

Similarly, for C57BL/6 mice, from the second week after vitamin D<sub>3</sub> treatment, body weight decreased to



a significantly lower level than the controls (Figure S2). It should be noted that weight loss during modeling is regarded as a sensitive indicator of the vitamin D<sub>3</sub>-induced calcification model.<sup>36,37</sup> In the vitamin D<sub>3</sub>-induced calcified mice, VC was shown in the aortic tissues by ARS staining (Figure 2A, left). Because the

mouse IL-29 gene is a pseudogene that does not encode an intact protein, we examined the expression of IFN $\lambda$ 2 (IL-28a) as the paralogue of the human IL-29 in mice,<sup>38</sup> as well as its specific receptor, IL-28R $\alpha$ . The results showed that both IL-28a and IL-28R $\alpha$  protein levels were higher in the aortic tissues of calcified mice

### Figure 1. IL-29 expression is elevated in calcified arteries from patients with CAD and CKD.

**A**, Quantification of IL-29 and BMP2 mRNA expression in the calcified carotid arteries from 4 patients with CAD, 4 patients with CKD, 6 noncalcified arteries, and a Pearson correlation between calcified arteries. The  $2^{-\Delta\Delta Ct}$  method was used, with GAPDH as an internal reference, to calculate the relative gene expression level. Data are mean $\pm$ SD. Statistical significance was tested using a 2-tailed unpaired *t* test. **B**, Representative images showing ARS staining for the lesions of calcification, as well as IL-29 and BMP2 protein expression on the lesions of the carotid arteries from 3 patients with CAD, 3 patients with CKD, and 3 noncalcified arteries as control. The magnification is  $\times 200$ . Arrows showed the calcification deposition. Data are mean $\pm$ SD. Statistical significance was calculated from an ordinary 1-way ANOVA with Tukey multiple comparisons test. ARS indicates alizarin red S; BMP2, bone morphogenetic protein 2; CAD, coronary artery disease; CKD, chronic kidney disease; GAPDH, glyceraldehyde-3-phosphate dehydrogenase; and IL-29, interleukin 29.

than those in the normal mice (Figure 2A, right). These data are based on both patients with CAD and CKD as well as calcified mice and indicate that IL-29 is involved in the VC pathogenesis.

### IL-28R $\alpha$ not IL-10R2 Is Mostly Expressed in the Aortic Tissues and VSMCs

To investigate whether IL-29 plays a role in VC formation via the key cell type, VSMCs, we examined the expression of the IL-29 receptor complex (IL-28R $\alpha$  and IL-10R2) in VSMCs, because both are the receptors for IL-29 to activate the VSMC activity. As shown by immunofluorescence, IL-28R $\alpha$  protein expression in the VSMCs (marked by  $\alpha$ -SMA) in the mouse aortic tissue was significantly higher than the IL-10R2 expression (Figure 2B). Accordingly, in isolated primary rat and human VSMCs, IL-28R $\alpha$  showed strong expression as compared with IL-10R2 either at the protein or mRNA level (Figure 2C and 2D). Thus, IL-28R $\alpha$ , not IL-10R2, is prominently expressed in VSMCs.

### IL-29 Inhibits the Proliferation of VSMCs

The specific activity of IL-29 was likely determined by the expression level of IL-28R $\alpha$ , as suggested by its abundance in the VSMCs. We therefore investigated the potential function of IL-29 on the VSMCs. First, primary RVSMCs were incubated with IL-29 (1, 10, or 100 ng/mL), and cell viability was monitored by the real-time cellular analysis in a real-time manner over 96 hours. The results showed IL-29 dose-dependently inhibited cell proliferation as evidenced by the cell index (Figure 3A), and this effect became significant after a 48-hour stimulation at the dosage of 100 ng/mL. Next, we examined the effect of IL-29 on cell apoptosis or migration, and found that the IL-29 treatment did not lead to a significant change in either apoptosis (Figure 3B) or migration of the cultured RVSMCs (Figure 3C).

### IL-29 Accelerates the Calcification of VSMCs

The phenotypic switch of VSMCs into osteogenic-like cells is a key process in VC associated with reduced VSMC proliferation.<sup>39,40</sup> To explore whether the inhibitory effect of IL-29 on the proliferation of VSMCs is

also present in the VC in our study, the effect of IL-29 on the VSMC calcification was examined in 2 calcification models, CaP- and OGM-induced VSMC calcification, respectively. Incubation of the primary RVSMCs both in the CaP medium for 3 to 5 days and OGM medium for 14 to 17 days induced cellular calcification. Significantly, the concurrent incubation with IL-29 at the concentration of 1, 10, or 100 ng/mL dose-independently augmented the calcification induced by CaP medium as shown by the red calcium nodes with the ARS staining, and the elevated optical density value after decalcification and calcium content quantitation (Figure 4A, upper). Similarly, in the osteogenic calcification condition, IL-29 (100 ng/mL) significantly enhanced the calcium deposition in RVSMCs compared with only calcium medium administration (Figure 4A, lower). Furthermore, the procalcification effect of IL-29 (100 ng/mL) was also observed in the primary cultured human VSMCs in the CaP condition (Figure 4B). These results support that IL-29 augments the VSMC calcification induced in different calcification conditions. Because of the stability and feasibility of the CaP medium to induce RVSMC calcification, we used this calcification model in the following studies.

### IL-29 Promotes the Rat Aortic Calcification Ex Vivo

To explore the procalcification effect of IL-29 in the whole artery segments, we used an organ culture system to induce the arterial calcification ex vivo. Rat aortic rings were treated with IL-29 (100 ng/mL) in the CaP medium for 6 days. After incubation with the CaP medium in the presence of IL-29, the aortic rings developed consistently more extensive calcification in the smooth muscle media than those aortic rings cultured in the CaP medium without IL-29, as shown by ARS staining (Figure 4C). Taken together, these observations indicate that IL-29 promotes the arterial calcification induced by the CaP medium ex vivo as well.

### IL-29 Induces Osteogenic Formation by VSMCs Under the Calcified Condition

We next sought to investigate whether IL-29 promotes the osteogenic differentiation of VSMCs in the calcified

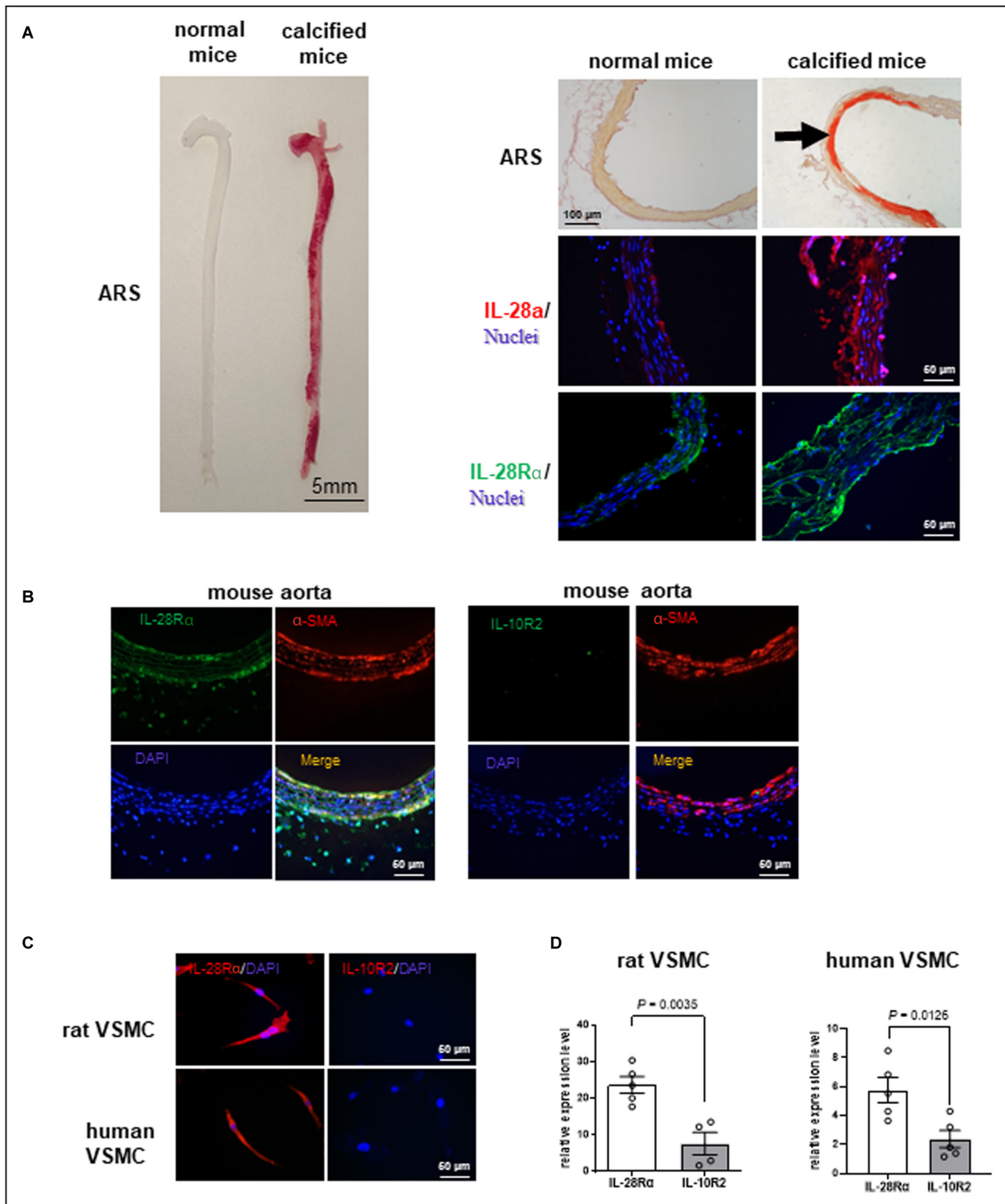


**Figure 2.** IL-28R $\alpha$  is highly expressed in calcified mice and specifically expressed in VSMCs.

**A**, Representative images of ARS staining for the calcification lesions ( $\times 200$ ), IL-28 $\alpha$  (red), as well as IL-28R $\alpha$  (green) expression in the aortic tissues of vitamin D<sub>3</sub>-induced calcified mice ( $\times 400$ ) ( $n=5$ ). Nuclei were stained with DAPI (blue). **B** and **C**, Representative images showing the protein expression of IL-28R $\alpha$  (green), IL-10R2 (green), and  $\alpha$ -SMA (red) in the mice aortic tissues, as well as IL-28R $\alpha$  (red) and IL-10R2 (red) in the primary rat and human VSMCs. Nuclei were stained with DAPI (blue). The magnification is  $\times 400$ . **D**, The mRNA levels of IL-28R $\alpha$  and IL-10R2 in the primary rat and human VSMCs. Data from a representative experiment were performed in 5 replicates and presented as mean $\pm$ SEM. Statistical significance was tested using a 2-tailed unpaired *t* test.  $\alpha$ -SMA indicates  $\alpha$ -smooth muscle actin; ARS, alizarin red S; DAPI, 4',6'-diamidino-2-phenylindole; IL-10R2, interleukin 10 receptor 2; IL-28 $\alpha$ , interleukin 28 $\alpha$ ; IL-28R $\alpha$ , interleukin 28 receptor  $\alpha$ ; and VSMC, vascular smooth muscle cell.



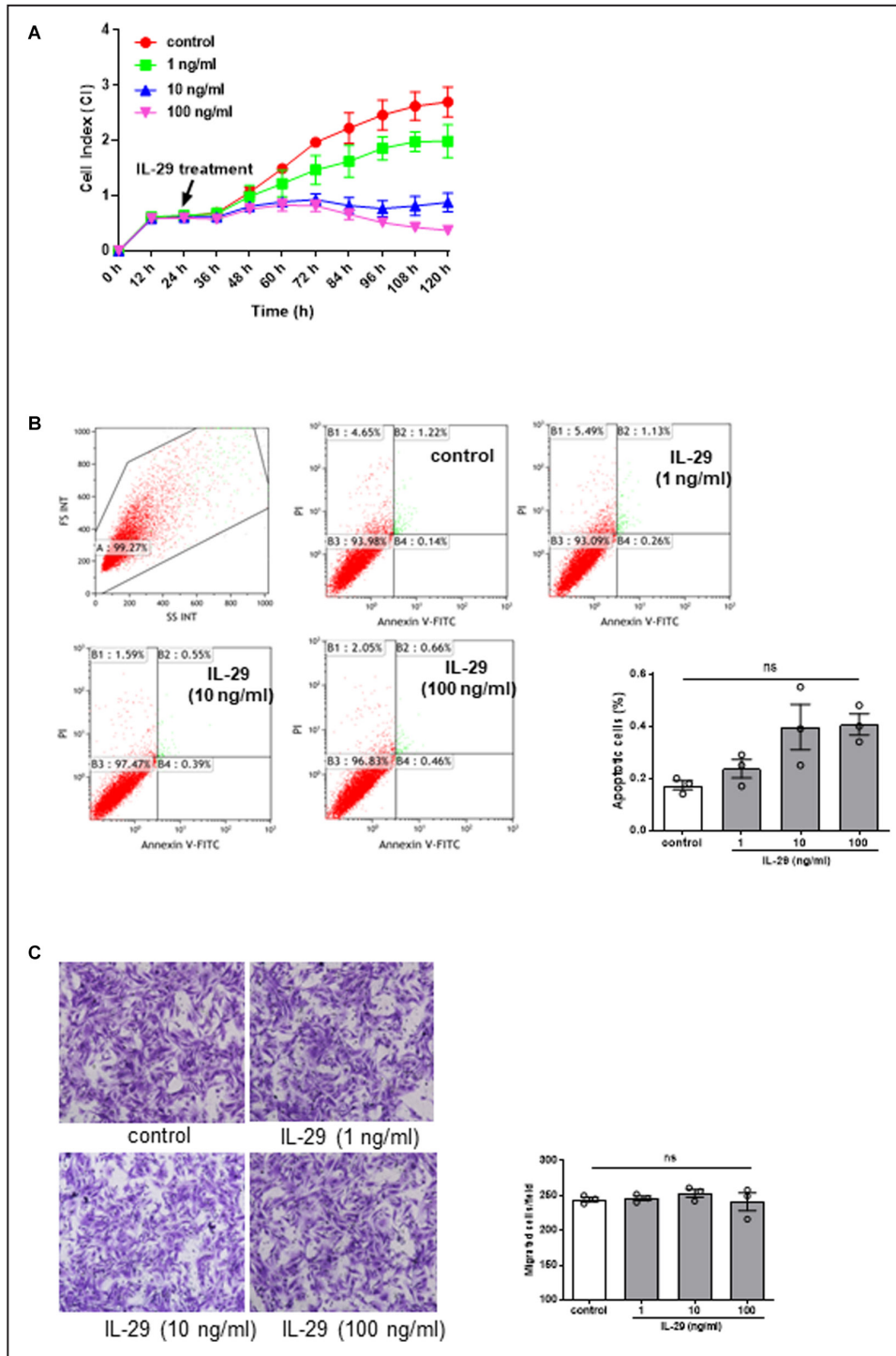
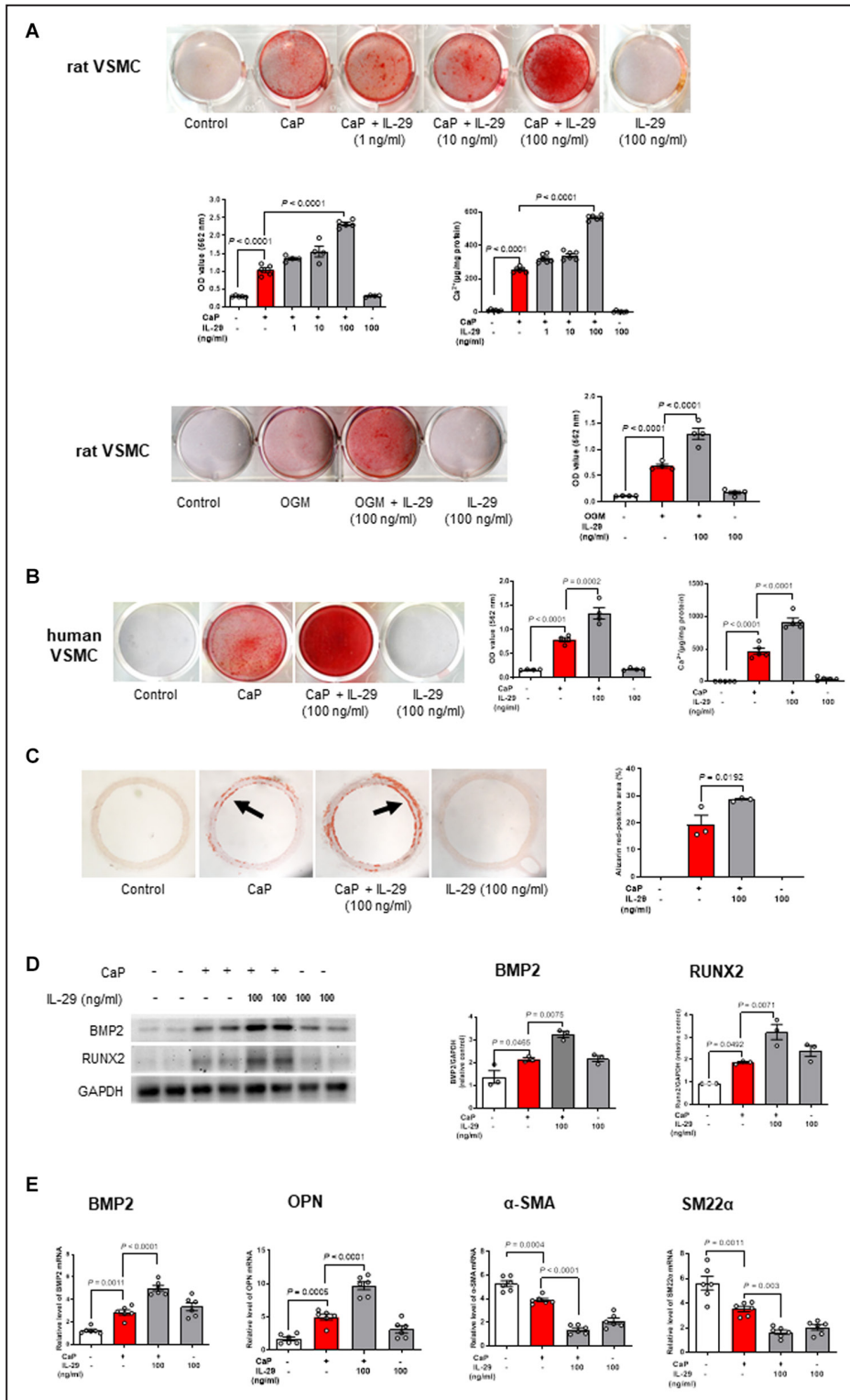


**Figure 3. IL-29 inhibits the proliferation of VSMCs without significant change in the apoptosis and migration.**

**A**, Proliferation of primary rat VSMCs (n=3) after treatment with IL-29 (1, 10, or 100 ng/mL) was monitored by real-time cellular analysis over 120 hours. Data from 1 representative experiment were performed in triplicate and presented as mean±SEM. **B** and **C**, Primary rat VSMCs was treated with different concentrations of IL-29 (1, 10, 100 ng/mL). The cell apoptosis was examined with flow cytometry at 48 hours, and the migration was determined with transwell analysis at 24 hours. Representative scattergrams show flow cytometry analysis for cell apoptosis, and micrographs show transwell assay for cell migration (×100). Data from 1 representative experiment performed in triplicate. Values are ±SEM. Statistical significance was calculated from ordinary 1-way ANOVA with Tukey multiple comparisons test. Annexin V-FITC indicates Annexin V-fluorescein isothiocyanate; Control, only medium treatment; IL-29, interleukin 29; ns, not significant; and VSMCs, vascular smooth muscle cells.



condition. IL-29 (100ng/mL) was added to the primary cultured RVSMCs in the CaP medium for 48 hours, and the osteogenic markers BMP2 and RUNX2 were examined by Western blots. As shown in Figure 4D, protein expressions of BMP2 and RUNX2 were significantly upregulated in the IL-29-treated RVSMCs

compared with the calcification medium control without IL-29. In addition, mRNA levels of osteogenic markers BMP2 and OPN were also elevated in the IL-29-treated (100ng/mL) RVSMCs with the CaP medium for 48 hours (Figure 4E). In contrast, mRNA levels of  $\alpha$ -SMA and SM22 $\alpha$ , the VSMC markers, were

#### Figure 4. IL-29 promotes the osteogenic differentiation and calcification in vitro and ex vivo.

**A and B**, Primary rat VSMCs were cultured with IL-29 (1, 10, or 100 ng/mL) in CaP medium for 3 days (upper) or IL-29 (100 ng/mL) administration in OGM medium for 17 days (lower), as well as IL-29 (100 ng/mL) treatment in primary human VSMCs in CaP medium for 3 days **B**. Representative photos of the ARS staining and quantified OD value were shown. In the other experimental set, cell supernatants and cell lysis were used for the quantification of calcium contents. Data from 1 representative experiment were performed in 4 to 6 replicates and shown as mean $\pm$ SEM. **C**, Rat aortic rings were exposed to CaP medium and IL-29 (100 ng/mL) for 6 days. Representative images and quantification of ARS staining for calcified areas by ImageJ software from 3 sections of each rat ( $n=3$ ) were displayed. The magnification is  $\times 40$ . Arrows indicated the calcified area. Values are mean $\pm$ SEM. **D**, Primary rat VSMCs were incubated with IL-29 (100 ng/mL) in the CaP condition for 48 hours. Representative Western blot images for BMP2 and RUNX2 protein expression were shown in duplicate each group (left), and relative expression of them to GAPDH were semiquantified (right). The cumulative data were from 3 independent experiments and expressed as mean $\pm$ SEM. **E**, Primary rat VSMCs were incubated with IL-29 (100 ng/mL) in the CaP condition for 48 hours. mRNA levels of VSMC osteogenic markers BMP2 and OPN, and VSMC phenotype markers  $\alpha$ -SMA and SM22 $\alpha$  were analyzed with real time polymerase chain reaction. Pooled data from 3 independent experiments were performed in duplicate and expressed as mean $\pm$ SEM. All of the statistical significance in this figure was calculated using ordinary 1-way ANOVA with Tukey multiple comparisons test.  $\alpha$ -SMA indicates  $\alpha$ -smooth muscle actin; ARS, alizarin red S; BMP2, bone morphogenetic protein 2; control, only medium treatment; GAPDH, glyceraldehyde-3-phosphate dehydrogenase; IL-29, interleukin 29; OD, optical density; OGM, osteogenic calcification medium; OPN, osteoprotegerin; RUNX2, Runt-related transcription factor 2; SM22 $\alpha$ , smooth muscle 22 $\alpha$ ; and VSMC, vascular smooth muscle cell.

decreased in the cultured RVSMCs in response to the IL-29 (100 ng/mL) treatment. These results support that IL-29 upregulates the osteogenic transformation by VSMCs under the calcification condition.

#### IL-29 or IL-28R $\alpha$ Neutralization Inhibits the Procalcification Effect of IL-29

To further demonstrate the effect of IL-29 in VC, we performed in vitro blocking experiments using the neutralization antibodies. RVSMCs were treated with IL-29 (100 ng/mL) with or without the presence of the IL-29 blocking antibodies (1 and 10  $\mu$ g/mL) in the CaP medium. As illustrated in [Figure 5A](#), the procalcification effect of IL-29 was markedly reduced after 3 days in the presence of IL-29 blocking antibodies at the concentration of 10  $\mu$ g/mL. The optical density value quantified after decalcification for the ARS staining showed a  $\sim$ 41.2% decrease compared with the control IL-29-treated group without the antibodies in the same CaP medium ( $P < 0.001$ ). Similarly, blocking of the specific receptor (IL-28R $\alpha$ ) of IL-29 in RVSMCs dose-dependently inhibited the increased calcification following the CaP and IL-29 (100 ng/mL) treatment ([Figure 5B](#)). Thus, the procalcifying effect of IL-29 in VSMCs is, at least in part, dependent on the specific receptor IL-28R $\alpha$ .

#### IL-29 Activates the JAK2/STAT3 Signaling Pathway During VSMC Calcification

It is known that IL-29 signals through the receptor complex (IL-28R $\alpha$  and IL-10R2) and activates the JAK-STAT-dependent or the mitogen-activated protein kinase-independent pathway to act against viral infection and tumor cells.<sup>41,42</sup> To elucidate the underlying mechanism of IL-29 during VSMC calcification, activation of the JAK-STAT and mitogen-activated protein kinase pathways was investigated by Western

blots. In RVSMCs, IL-29 (100 ng/mL) significantly activated the JAK2 phosphorylation at 30 or 60 minutes compared with the control CaP group without IL-29 ([Figure 6A](#)). More importantly, IL-29 (100 ng/mL) prominently stimulated the activation of STAT3 (Tyr705) at 30 or 60 minutes in RVSMCs, without affecting the phosphorylation of STAT2 (Tyr690), STAT5 (Tyr694), and STAT6 (Tyr641) ([Figure 6B](#)). In addition, phosphorylated STAT1 (Tyr701) and STAT4 (Tyr693) were not detectable in these cells. The mitogen-activated protein kinase signaling molecules phosphorylated p38, ERK, and JNK remained at the same levels in the cultured RVSMCs following the IL-29 treatment (100 ng/mL) for 30 or 60 minutes as compared with the CaP controls without IL-29 ([Figure 6C](#)). These results support that a specific JAK2/STAT3 signaling pathway contributes to the IL-29-mediated calcification in VSMCs.

#### Inhibition of JAK2/STAT3 Pathway Reduces the IL-29-Dependent VSMC Calcification

We conducted antagonistic experiments to define whether the procalcifying effect of IL-29 was by activating the JAK2/STAT3 pathway. To this end, RVSMCs were treated with IL-29 with or without the presence of a JAK2 or STAT3 inhibitor in the CaP medium for 3 days. As shown by the ARS staining in [Figure 7A](#) and [7B](#), both JAK2 antagonist (fedratinib, 1  $\mu$ M) and STAT3 antagonist (niclosamide, 10  $\mu$ g/mL) partially reduced the extent of calcium deposition induced by IL-29 under the CaP condition. Additionally, the JAK2 or STAT3 antagonist significantly reduced the expression of BMP2 proteins in the CaP-treated RVSMCs with the presence of IL-29 (100 ng/mL) as determined by Western blot ([Figure 7C](#) and [7D](#)). Together, these results document that inhibition of JAK2/STAT3 pathway alleviates the osteogenic transformation and

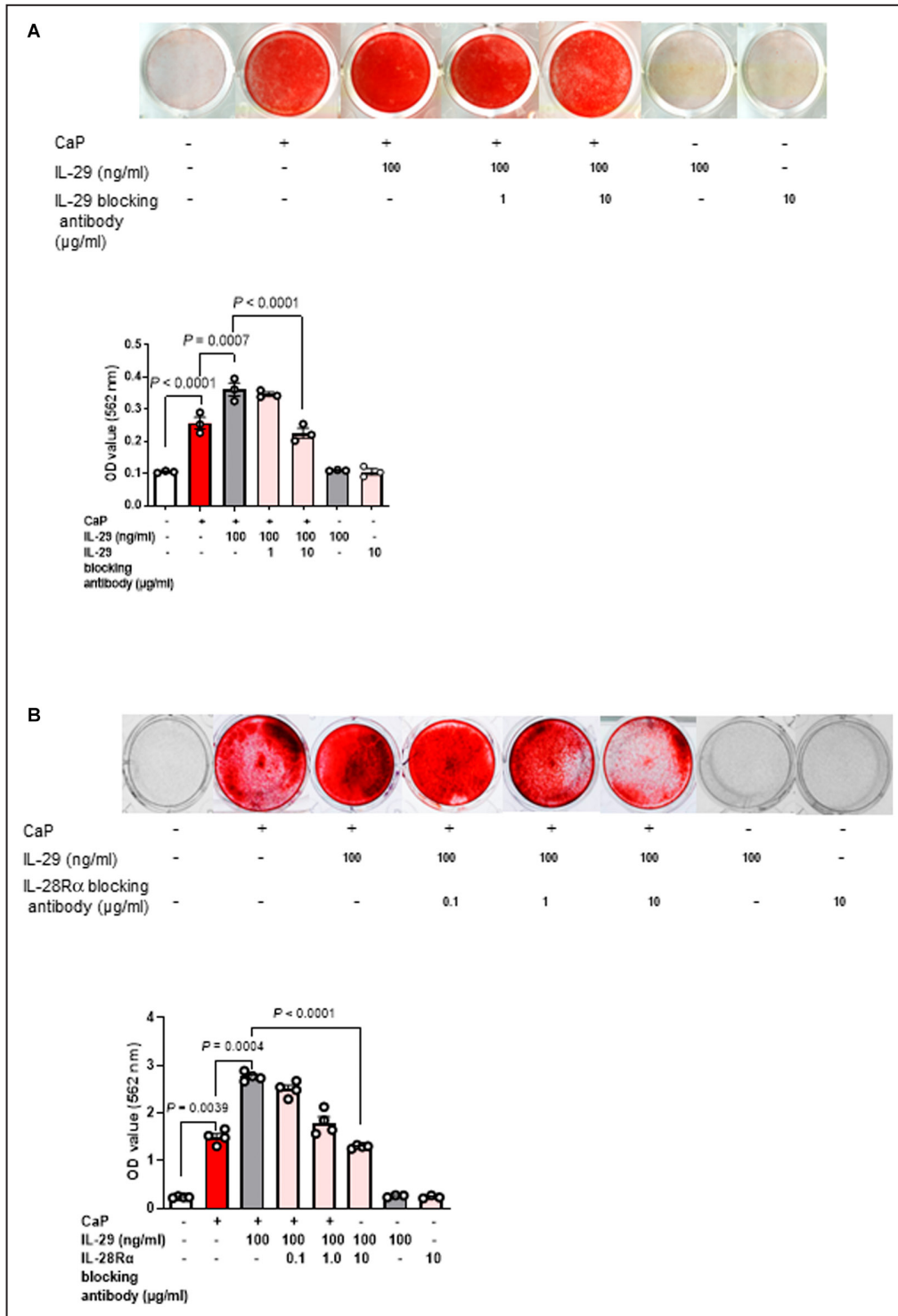


**Figure 5. Blocking IL-29 or IL-28Rα inhibits the procalcification effect of IL-29.**

**A** and **B**, Primary rat VSMCs were cultured with IL-29 (100ng/mL) in the presence of IL-29 neutralization antibody (1 and 10 μg/mL) or IL-28Rα neutralization antibody (0.1, 1, or 10 μg/mL) in the CaP condition for 3 days. Representative images of ARS staining are displayed. The cumulative data for OD value were from 1 representative experiment performed in triplicates or quadruplicates and expressed as mean±SEM. Statistical significance was tested using ordinary 1-way ANOVA with Tukey multiple comparisons test (**A**) and Brown-Forsythe ANOVA followed by Dunnett T3 multiple comparisons test (**B**). ARS indicates alizarin red S; IL-28Rα, interleukin 28 receptor α; IL-29, interleukin 29; CaP, calcification medium; OD, optical density; and VSMC, vascular smooth muscle cell.

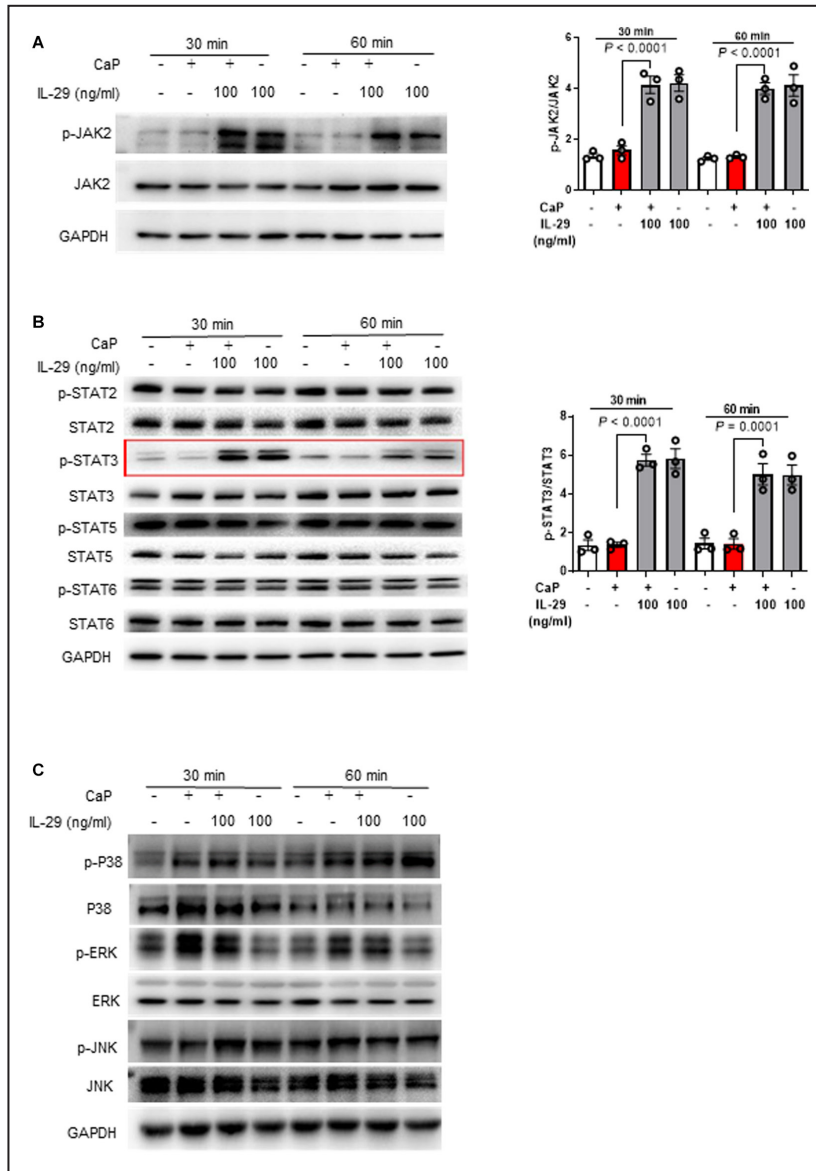


**Figure 6. IL-29 selectively activates JAK2/STAT3 signaling pathway in VSMC calcification.**

**A and B**, Representative Western blots and semiquantitative analysis for the change of JAK2/STAT pathways in primary rat VSMCs treated with IL-29 (100ng/mL) in the CaP condition for 30 and 60 minutes, respectively. p-STAT1/STAT1 and p-STAT4/STAT4 were not detected in this experiment. The cumulative data were from 3 independent experiments and expressed as mean±SEM. Statistical significance was calculated from ordinary 1-way ANOVA with Tukey multiple comparisons test. **C**, Representative Western blots for the change of MAPK pathway. No obvious changes were observed after IL-29 treatment in CaP condition compared with only CaP medium-treated group. CaP indicates calcification medium; ERK, extracellular regulated protein kinase; GAPDH, glyceraldehyde-3-phosphate dehydrogenase; IL-29, interleukin 29; JAK2, janus kinase 2; JNK, c-Jun N-terminal kinase; MAPK, mitogen-activated protein kinase; P38, p38 mitogen activated protein kinase; p-ERK, phospho-ERK; p-JAK2, phospho-JAK2; p-JNK, phospho-JNK; p-P38, phospho-P38; p-STAT1, phospho-STAT1; p-STAT2, phospho-STAT2; p-STAT3, phospho-STAT3; p-STAT4, phospho-STAT4; p-STAT5, phospho-STAT5; p-STAT6, phospho-STAT6; STAT1, signal transducer and activator of transcription 1; STAT2, signal transducer and activator of transcription 2; STAT3, signal transducer and activator of transcription 3; STAT4, signal transducer and activator of transcription 4; STAT5, signal transducer and activator of transcription 5; STAT6, signal transducer and activator of transcription 6; and VSMC, vascular smooth muscle cell.

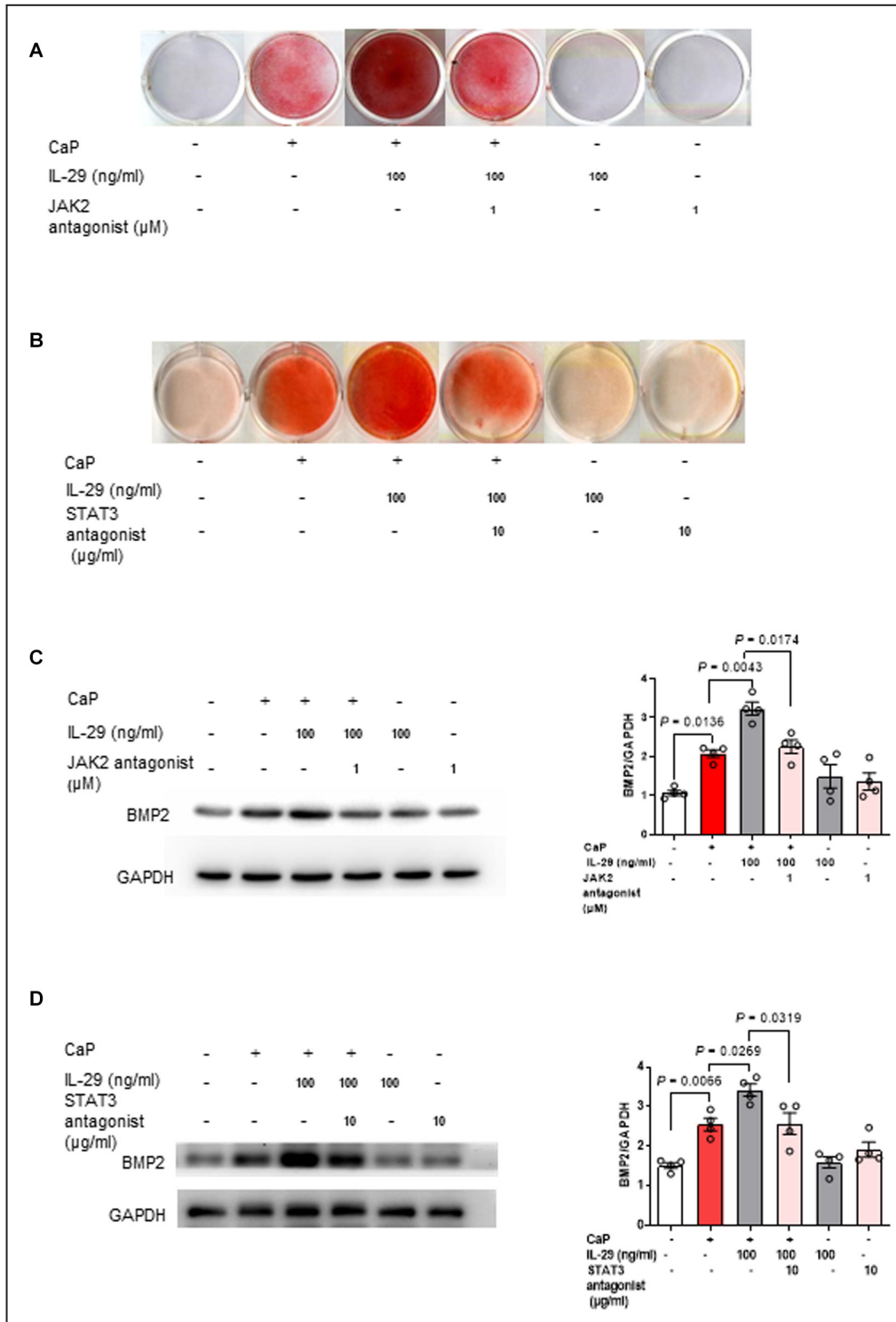


**Figure 7. JAK2 or STAT3 antagonist reduces the procalcification effect of IL-29 and BMP2 expression.** **A** and **B**, Primary rat VSMCs were treated with IL-29 (100 ng/mL) with or without the presence of JAK2 antagonist (fedratinib, 1  $\mu$ M) or STAT3 antagonist (niclosamide, 10  $\mu$ g/mL) in the CaP condition for 3 days. Representative images of ARS staining for calcium deposition were shown. **C** and **D**, Representative Western blots and semiquantitative analysis showed the effect of JAK2 or STAT3 antagonist on BMP2 protein expression. The cumulative data were from 4 independent experiments and expressed as mean  $\pm$  SEM. Statistical significance was calculated from ordinary 1-way ANOVA with Tukey multiple comparisons test. ARS indicates alizarin red S; BMP2, bone morphogenetic protein 2; CaP, calcification medium; GAPDH, glyceraldehyde-3-phosphate dehydrogenase; IL-29, interleukin 29; JAK2, janus kinase 2; STAT3, signal transducer and activator of transcription 3; and VSMC, vascular smooth muscle cell.

calcification of VSMCs mediated by IL-29 under the CaP condition.

## DISCUSSION

The present study, for the first time, demonstrates IL-29 as a proinflammatory cytokine promoting the VSMC osteogenic transformation and calcification under the CaP condition. We further show that binding of IL-29 to its receptor IL-28R $\alpha$  enhances the activation of JAK2/STAT3 to upregulate BMP2 in VSMCs to promote their calcification and osteogenic transformation. Our data suggest that inhibition of IL-29 signaling using synthetic, small-molecule inhibitors may be a useful strategy to reduce VC in patients.

VSMCs transdifferentiation to osteochondrogenic phenotype is the primary process of VC, and inflammatory cytokines have been shown to favor it.<sup>7</sup> IL-29 is a newly discovered cytokine belonging to type III interferon,<sup>22</sup> and recently its effect in inflammatory autoimmune diseases has been revealed in our previous studies and other groups.<sup>25,30,33</sup> In the present study, we first observed that IL-29 mRNA expression was significantly higher in the calcified carotid arteries from patients with CAD and CKD than noncalcified carotid arteries, and positively correlated with BMP2 (one of the osteogenic markers) expression. In protein level, IL-29 and BMP2 were abundantly expressed and colocalized at or around the calcified regions in the carotid arteries from patients with CAD and CKD (Figure 1). Interestingly, the higher mRNA and protein expression of IL-29 was detected in calcified carotid arteries not only from patients with CAD but also patients with CKD, which strongly suggest that IL-29 may play a pivotal role in the VC process, albeit the calcification occurs in the intimal or medial layer of the vessels. Considering the pathological deposition of calcium phosphate mineral in arteries is a common consequence of VC in CVD and CKD, in the present study, we used the vitamin D<sub>3</sub>-induced calcified mice and the CaP medium (1.5 mM calcium and 2.0 mM phosphate)-induced cell calcification model to mimic the VC process as previously used in our laboratory.<sup>34</sup> Consistent with the aberrant expression of IL-29 in human calcified arteries, we further observed the higher levels of IL-28 $\alpha$  and its specific receptor, IL-28R $\alpha$ , in the aortas of vitamin D<sub>3</sub>-induced calcified mice than those in normal mice (Figure 2A). Taken together, these observations are promising, suggesting that IL-29 is closely related to the VC process involved in calcification-associated diseases. However, it cannot exclude the possible effect of vitamin D<sub>3</sub> intoxication on altering the physiological and pathophysiological mechanism of VC in this calcification mice model; therefore, further animal experiments,

including an atherosclerotic calcification model, are required to investigate the role of IL-29 in VC.

VC is an active and tightly regulated process, principally driven by the VSMCs. Cytokines released by inflammatory cells (such as macrophages) can induce VSMCs apoptosis, migration, or phenotype transdifferentiation, contributing to triggering or exacerbating the VC process.<sup>10,18</sup> We performed in vitro experiments to explore whether IL-29 affects VSMCs function and phenotype alterations via its proinflammatory mechanism. The selective IL-28R $\alpha$  (the specific receptor of IL-29) expression pattern limits the responsiveness of IL-29 in restricted cells and tissues<sup>24</sup>; notably, in this study we detected marked expression of IL-28R $\alpha$  not only in the VSMCs located in the mouse aortic arteries (Figure 2B), but also in primary cultured human and rat VSMCs (Figure 2C and 2D). In contrast, rare or low IL-10R2 expression was detected in the same tissues or cells. Based on our knowledge, this is the first report about IL-29 receptor expression in VSMCs. The abundant expression of IL-28R $\alpha$  in VSMCs strongly suggests VSMCs may respond to the aberrantly expressed IL-29 in vascular microenvironment.

Growing evidence suggests that decreased VSMC proliferation is accompanied by gain of osteo/chondrogenic phenotype in vitro and in calcified lesions.<sup>8</sup> In this study, IL-29 treatment remarkably inhibited the proliferation of primary rat VSMCs in a dose-dependent manner (Figure 3A), implying this cellular response may relate to VC process. We observed that IL-29 significantly enhanced CaP medium or osteogenic medium-induced VSMC calcification and osteo/chondrogenic transdifferentiation both in primary rat and human VSMCs in vitro as well as rat aortic ring segments ex vivo in the CaP condition (Figure 4). Accordingly, at the molecular level, we also found the increased mRNA expression of osteogenic markers (BMP2, RUNX2, and OPN) in IL-29-stimulated VSMCs under calcification condition, whereas markers of the VSMC phenotype including  $\alpha$ -SMA and SM22 $\alpha$  were decreased. Moreover, treatments with IL-29 or IL-28R $\alpha$  neutralization antibody strongly blunted the procalcifying effect of IL-29 in calcification conditions (Figure 5). Based on our present in vitro data, it is reasonable to believe that IL-29 binding to its specific receptor, IL-28R $\alpha$ , aggravates VSMC calcification and osteogenic transdifferentiation. The process of VC is now considered similar to bone formation, especially in terms of mineral composition and osteoblast differentiation. Notably, we and other groups recently proved a novel effect of IL-29 on inflammatory bone loss via secretion of proinflammatory cytokines (tumor necrosis factor- $\alpha$ , IL-1 $\beta$ , and IL-6).<sup>31,33</sup> Thus, it is not surprising that the inflammatory role of IL-29 might be involved in the VC process in the current study.

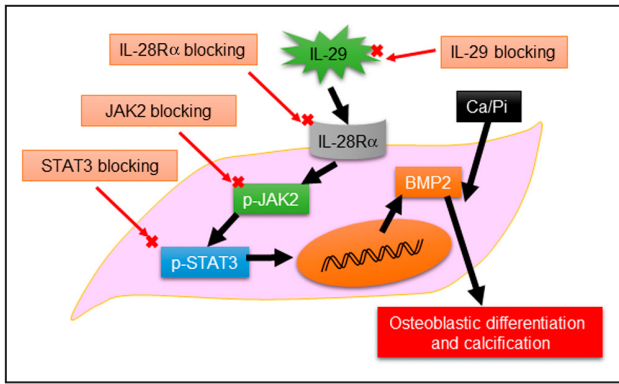


**Figure 8. Schematic illustration of the effect of IL-29 on VSMC calcification process and possible blocking strategies.** IL-29 accelerates the osteogenic differentiation and calcification of VSMCs under the CaP condition. This process can be interrupted by blocking the binding of IL-29/IL-28R $\alpha$  or activation of JAK2/STAT3 pathway. BMP2 indicates bone morphogenetic protein 2; Ca, calcium; CaP, calcification medium; IL-28R $\alpha$ , interleukin 28 receptor  $\alpha$ ; IL-29, interleukin 29; JAK2, janus kinase 2; Pi, inorganic phosphate; p-JAK2, phospho-JAK2; p-STAT3, phospho-STAT3; STAT3, signal transducer and activator of transcription 3; and VSMC, vascular smooth muscle cell.

To further investigate the mechanism by which IL-29 promotes VC process, we observed the possible intracellular signaling pathways involved. JAK/STAT signaling pathways were upregulated in calcified aortas and mediated osteogenic transformation of VSMCs.<sup>13,43</sup> Importantly, JAK2 activation was recently found to play a key role in the activity of IL-29.<sup>44</sup> Consistent with the above findings, we found IL-29 stimulated the phosphorylation of JAK2 in VSMCs under calcification conditions and its downstream molecule STAT3, which was the only highly phosphorylated one among all of the STAT members (Figure 6). Whereas in the present study, IL-29 cannot affect the activation of mitogen-activated protein kinase pathway in VSMCs, although IL-29 activates them in other cells.<sup>44</sup> In spite of the above data showing that IL-29 specially promotes JAK2/STAT3 phosphorylation in VSMCs after short-term treatment (30 and 60 minutes), it needs to further examine if the procalcifying effect of IL-29 is modulated by the activated JAK2/STAT3 pathway in the VC process.

Therefore, we investigated the effect of IL-29 on VC formation after blocking JAK2/STAT3 signaling in vitro. Expectedly, JAK2 or STAT3 antagonist distinctly blunted the increased numbers of calcification nodules induced by IL-29 treatment after 3 days in the CaP medium (Figure 7). Meanwhile, Western blot further revealed that the 2 antagonists were able to block IL-29-induced upregulation of osteogenic maker BMP2. BMP2 is widely accepted as a crucial molecule in the osteogenic differentiation and pathogenesis of VC. We also detected enriched colocalization of IL-29 and BMP2 in human calcified arteries as well as increased BMP2

level in IL-29-stimulated VSMCs. Taken together, the above results suggest that IL-29 upregulated BMP2 expression by increasing JAK2/STAT3 phosphorylation, thereby promoting VSMC osteogenic transformation and calcification. The detailed mechanism behind this effect warrants further investigation.

In summary, our study suggests that IL-29 in calcified lesions binds to the specific receptor IL-28R $\alpha$  on VSMCs, at least partly, activating the JAK2/STAT3 signaling pathway to upregulate BMP2 expression and promote the osteogenic transformation and calcification by VSMCs (Figure 8). This new evidence for the proinflammatory role of IL-29 involved in VC warrants further investigations on its inhibition via blocking IL-29/IL-28R $\alpha$  and/or JAK2/STAT3 as a new therapeutic strategy for VC-related diseases.

## ARTICLE INFORMATION

Received June 21, 2022; accepted September 19, 2022.

### Affiliations

Department of Cardiology (N.H., Z.Z., F.Z., Y.L., C.L., F.W.); Department of Vascular Surgery (R.H., J.Z.); Department of Cardiovascular Surgery (R.Z.) and Department of Rheumatology, The First Affiliated Hospital of Nanjing Medical University, Nanjing, Jiangsu Province, China (L.W., L.X., W.T.).

### Acknowledgments

N.H., Z.Z., and F.Z. performed cell and molecular experiments. L.X. and L.W. launched the animal experiments. Y.L., R.H., J.Z., and R.Z. collected samples. W.T. and F.W. designed the study and interpreted the data. C.L. revised the article. All authors read and approved the final article.

### Sources of Funding

This project was sponsored by the grants from the National Natural Science Foundation of China (numbers 81971533, 81971532, 82171794, 82170351).

### Disclosures

None.

### Supplemental Material

Data S1  
Table S1–S2  
Figures S1–S2

## REFERENCES

- Giachelli CM. Vascular calcification mechanisms. *J Am Soc Nephrol*. 2004;15:2959–2964. doi: 10.1097/01.ASN.0000145894.57533.C4
- Shao JS, Sierra OL, Cohen R, Mechem RP, Kovacs A, Wang J, Distelhorst K, Behrmann A, Halstead LR, Towler DA. Vascular calcification and aortic fibrosis: a bifunctional role for osteopontin in diabetic arteriosclerosis. *Arterioscler Thromb Vasc Biol*. 2011;31:1821–1833. doi: 10.1161/ATVBAHA.111.230011
- Jensky NE, Criqui MH, Wright MC, Wassel CL, Brody SA, Allison MA. Blood pressure and vascular calcification. *Hypertension*. 2010;55:990–997. doi: 10.1161/HYPERTENSIONAHA.109.147520
- Wu M, Rementer C, Giachelli CM. Vascular calcification: an update on mechanisms and challenges in treatment. *Calcif Tissue Int*. 2013;93:365–373. doi: 10.1007/s00223-013-9712-z
- Moe SM, Chen NX. Pathophysiology of vascular calcification in chronic kidney disease. *Circ Res*. 2004;95:560–567. doi: 10.1161/01.RES.0000141775.67189.98
- Kahn MR, Robbins MJ, Kim MC, Fuster V. Management of cardiovascular disease in patients with kidney disease. *Nat Rev Cardiol*. 2013;10:261–273. doi: 10.1038/nrcardio.2013.15



7. Sage AP, Tintut Y, Demer LL. Regulatory mechanisms in vascular calcification. *Nat Rev Cardiol*. 2010;7:528–536. doi: 10.1038/nrcardio.2010.115
8. Durham AL, Speer MY, Scatena M, Giachelli CM, Shanahan CM. Role of smooth muscle cells in vascular calcification: implications in atherosclerosis and arterial stiffness. *Cardiovasc Res*. 2018;114:590–600. doi: 10.1093/cvr/cvy010
9. Demer LL, Tintut Y. Vascular calcification: pathobiology of a multifaceted disease. *Circulation*. 2008;117:2938–2948. doi: 10.1161/CIRCULATIONAHA.107.743161
10. Leopold JA. Vascular calcification: mechanisms of vascular smooth muscle cell calcification. *Trends Cardiovasc Med*. 2015;25:267–274. doi: 10.1016/j.tcm.2014.10.021
11. Lee SJ, Lee IK, Jeon JH. Vascular calcification-new insights into its mechanism. *Int J Mol Sci*. 2020;21:2685. doi: 10.3390/ijms21082685
12. Pustlauk W, Westhoff TH, Claeys L, Roch T, Geissler S, Babel N. Induced osteogenic differentiation of human smooth muscle cells as a model of vascular calcification. *Sci Rep*. 2020;10:5951. doi: 10.1038/s41598-020-62568-w
13. Han Y, Zhang J, Huang S, Cheng N, Zhang C, Li Y, Wang X, Liu J, You B, Du J. MicroRNA-223-3p inhibits vascular calcification and the osteogenic switch of vascular smooth muscle cells. *J Biol Chem*. 2021;296:100483. doi: 10.1016/j.jbc.2021.100483
14. Liu Y, Drozdov I, Shroff R, Beltran LE, Shanahan CM. Prelamin A accelerates vascular calcification via activation of the DNA damage response and senescence-associated secretory phenotype in vascular smooth muscle cells. *Circ Res*. 2013;112:e99–e109. doi: 10.1161/CIRCRESAHA.111.300543
15. Shanahan CM, Furmanik M. Endoplasmic reticulum stress in arterial smooth muscle cells: a novel regulator of vascular disease. *Curr Cardiol Rev*. 2017;13:94–105.
16. Wen C, Yang X, Yan Z, Zhao M, Yue X, Cheng X, Zheng Z, Guan K, Dou J, Xu T, et al. Nalp3 inflammasome is activated and required for vascular smooth muscle cell calcification. *Int J Cardiol*. 2013;168:2242–2247. doi: 10.1016/j.ijcard.2013.01.211
17. Frauscher B, Kirsch AH, Schabhtull C, Schweighofer K, Ketszeri M, Pollheimer M, Dragun D, Schroder K, Rosenkranz AR, Eller K, et al. Autophagy protects from uremic vascular media calcification. *Front Immunol*. 2018;9:1866. doi: 10.3389/fimmu.2018.01866
18. Shobeiri N, Bendeck MP. Interleukin-1beta is a key biomarker and mediator of inflammatory vascular calcification. *Arterioscler Thromb Vasc Biol*. 2017;37:179–180. doi: 10.1161/ATVBAHA.116.308724
19. New SE, Aikawa E. Molecular imaging insights into early inflammatory stages of arterial and aortic valve calcification. *Circ Res*. 2011;108:1381–1391. doi: 10.1161/CIRCRESAHA.110.234146
20. Tintut Y, Patel J, Parhami F, Demer LL. Tumor necrosis factor-alpha promotes in vitro calcification of vascular cells via the camp pathway. *Circulation*. 2000;102:2636–2642. doi: 10.1161/01.CIR.102.21.2636
21. Aikawa E, Nahrendorf M, Figueiredo JL, Swirski FK, Shtatland T, Kohler RH, Jaffer FA, Aikawa M, Weissleder R. Osteogenesis associates with inflammation in early-stage atherosclerosis evaluated by molecular imaging in vivo. *Circulation*. 2007;116:2841–2850. doi: 10.1161/CIRCULATIONAHA.107.732867
22. Sheppard P, Kindsvogel W, Xu W, Henderson K, Schlutsmeyer S, Whitmore TE, Kuestner R, Garrigues U, Birks C, Roraback J, et al. IL-28, IL-29 and their class II cytokine receptor IL-28R. *Nat Immunol*. 2003;4:63–68. doi: 10.1038/ni873
23. Prokunina-Olsson L, Muchmore B, Tang W, Pfeiffer RM, Park H, Dickensheets H, Hergott D, Porter-Gill P, Mumy A, Kohaar I, et al. A variant upstream of ifnl3 (il28b) creating a new interferon gene ifnl4 is associated with impaired clearance of hepatitis c virus. *Nat Genet*. 2013;45:164–171. doi: 10.1038/ng.2521
24. Lazear HM, Schoggins JW, Diamond MS. Shared and distinct functions of type I and type III interferons. *Immunity*. 2019;50:907–923. doi: 10.1016/j.immuni.2019.03.025
25. Wang F, Xu L, Feng X, Guo D, Tan W, Zhang M. Interleukin-29 modulates proinflammatory cytokine production in synovial inflammation of rheumatoid arthritis. *Arthritis Res Ther*. 2012;14:R228. doi: 10.1186/ar4067
26. Commins S, Steinke JW, Borish L. The extended IL-10 superfamily: IL-10, IL-19, IL-20, IL-22, IL-24, IL-26, IL-28, and IL-29. *J Allergy Clin Immunol*. 2008;121:1108–1111. doi: 10.1016/j.jaci.2008.02.026
27. Sommereyns C, Paul S, Staeheli P, Michiels T. IFN-lambda (IFN-lambda) is expressed in a tissue-dependent fashion and primarily acts on epithelial cells in vivo. *PLoS Pathog*. 2008;4:e1000017. doi: 10.1371/journal.ppat.1000017
28. da Rocha Junior LF, Branco Pinto Duarte AL, de Melo Rego MJB, de Almeida AR, de Melo Vilar K, de Lima HD, Tavares Dantas A, de Ataíde Mariz H, da Rocha Pitta I, da Rocha Pitta MG. Sensitivity and specificity of interleukin 29 in patients with rheumatoid arthritis and other rheumatic diseases. *Immunol Lett*. 2020;220:38–43. doi: 10.1016/j.imlet.2020.01.004
29. Oke V, Brauner S, Larsson A, Gustafsson J, Zickert A, Gunnarsson I, Svenungsson E. IFN-λ1 with Th17 axis cytokines and IFN-α define different subsets in systemic lupus erythematosus (SLE). *Arthritis Res Ther*. 2017;19:139. doi: 10.1186/s13075-017-1344-7
30. Wu Q, Yang Q, Lourenco E, Sun H, Zhang Y. Interferon-lambda1 induces peripheral blood mononuclear cell-derived chemokines secretion in patients with systemic lupus erythematosus: its correlation with disease activity. *Arthritis Res Ther*. 2011;13:R88. doi: 10.1186/ar3363
31. Peng Q, Luo A, Zhou Z, Xuan W, Qiu M, Wu Q, Xu L, Kong X, Zhang M, Tan W, et al. Interleukin 29 inhibits rankl-induced osteoclastogenesis via activation of jnk and stat, and inhibition of nf-kappab and nfatc1. *Cytokine*. 2019;113:144–154. doi: 10.1016/j.cyto.2018.06.032
32. Chen Y, Wang Y, Tang R, Yang J, Dou C, Dong Y, Sun D, Zhang C, Zhang L, Tang Y, et al. Dendritic cells-derived interferon-lambda1 ameliorated inflammatory bone destruction through inhibiting osteoclastogenesis. *Cell Death Dis*. 2020;11:414. doi: 10.1038/s41419-020-2612-z
33. Deng Z, Hu W, Ai H, Chen Y, Dong S. The dramatic role of ifn family in aberrant inflammatory osteolysis. *Curr Gene Ther*. 2021;21:112–129. doi: 10.2174/1566523220666201127114845
34. Shi W, Lu J, Li J, Qiu M, Lu Y, Gu J, Kong X, Sun W. Piperlongumine attenuates high calcium/phosphate-induced arterial calcification by preserving p53/pten signaling. *Front Cardiovasc Med*. 2020;7:625215. doi: 10.3389/fcvm.2020.625215
35. Xu L, Feng X, Tan W, Gu W, Guo D, Zhang M, Wang F. IL-29 enhances toll-like receptor-mediated IL-6 and IL-8 production by the synovial fibroblasts from rheumatoid arthritis patients. *Arthritis Res Ther*. 2013;15:R170. doi: 10.1186/ar4357
36. Price PA, Faus SA, Williamson MK. Warfarin-induced artery calcification is accelerated by growth and vitamin D. *Arterioscler Thromb Vasc Biol*. 2000;20:317–327. doi: 10.1161/01.ATV.20.2.317
37. Sisley SR, Arble DM, Chambers AP, Gutierrez-Aguilar R, He Y, Xu Y, Gardner D, Moore DD, Seeley RJ, Sandoval DA. Hypothalamic vitamin D improves glucose homeostasis and reduces weight. *Diabetes*. 2016;65:2732–2741. doi: 10.2337/db16-0309
38. Lasfar A, Lewis-Antes A, Smirnov SV, Anantha S, Abushahba W, Tian B, Reuhl K, Dickensheets H, Sheikh F, Donnelly RP, et al. Characterization of the mouse ifn-lambda ligand-receptor system: IFN-lambdas exhibit antitumor activity against B16 melanoma. *Cancer Res*. 2006;66:4468–4477. doi: 10.1158/0008-5472.CAN-05-3653
39. Furmanik M, Chatrou M, van Gorp R, Akbulut A, Willems B, Schmidt H, van Eys G, Bochaton-Piallat ML, Proudfoot D, Biessen E, et al. Reactive oxygen-forming nox5 links vascular smooth muscle cell phenotypic switching and extracellular vesicle-mediated vascular calcification. *Circ Res*. 2020;127:911–927. doi: 10.1161/CIRCRESAHA.119.316159
40. Alexander MR, Owens GK. Epigenetic control of smooth muscle cell differentiation and phenotypic switching in vascular development and disease. *Annu Rev Physiol*. 2012;74:13–40. doi: 10.1146/annurev-physiol-012110-142315
41. Brand S, Beigel F, Olszak T, Zitzmann K, Eichhorst ST, Otte JM, Diebold J, Diepolder H, Adler B, Auernhammer CJ, et al. IL-28a and IL-29 mediate antiproliferative and antiviral signals in intestinal epithelial cells and murine cmv infection increases colonic IL-28A expression. *Am J Physiol Gastrointest Liver Physiol*. 2005;289:G960–G968. doi: 10.1152/ajpgi.00126.2005
42. Doyle SE, Schreckhise H, Khuu-Duong K, Henderson K, Rosler R, Storey H, Yao L, Liu H, Barahmand-pour F, Sivakumar P, et al. Interleukin-29 uses a type 1 interferon-like program to promote antiviral responses in human hepatocytes. *Hepatology*. 2006;44:896–906. doi: 10.1002/hep.21312
43. Yang T, Guo L, Chen L, Li J, Li Q, Pi Y, Zhu J, Zhang L. A novel role of FKN/CX3CR1 in promoting osteogenic transformation of vsmcs and atherosclerotic calcification. *Cell Calcium*. 2020;91:102265. doi: 10.1016/j.ceca.2020.102265
44. Zhou Z, Hamming OJ, Ank N, Paludan SR, Nielsen AL, Hartmann R. Type III interferon (IFN) induces a type I IFN-like response in a restricted subset of cells through signaling pathways involving both the Jak-STAT pathway and the mitogen-activated protein kinases. *J Virol*. 2007;81:7749–7758. doi: 10.1128/JVI.02438-06

## **SUPPLEMENTAL MATERIAL**

## **Data S1. Supplemental Methods**

### **Alizarin red S staining and OD quantification**

As to ARS staining for cells, VSMCs in 24-well plate were washed in PBS for 3 times and fixed with 4% PFA for 10 minutes. The wells were washed with ddH<sub>2</sub>O, stained with 0.2% ARS (pH 4.2) solution for 3-5 minutes at room temperature. After rinsing with ddH<sub>2</sub>O, the plates were photographed. To quantify ARS contents, cells after staining were decalcified in 10% cetylpyridinium chloride solution for 5-10 minutes and their absorbance were measured at wavelength 562 nm using a multi-plate reader (BioTek Synergy 2, VT, USA).

As to ARS staining for the whole aortas, the aortas were washed in PBS for 3 times and fixed with 4% PFA for 6 hours. The vessels were washed with ddH<sub>2</sub>O, stained with 0.2% ARS (pH 8.3) solution for 1 hours at room temperature. After rinsing with Bleach solution for 12 hours, the aortas were washed and photographed. Bleach solution was made by mixing just before use equal volumes of 3% H<sub>2</sub>O<sub>2</sub> and 4% KOH to give final concentration of 1.5% H<sub>2</sub>O<sub>2</sub> and 2% KOH.

As to ARS staining for frozen sections, the sections were recovered to room temperature, fixed with 4% PFA for 15 minutes and stained with 0.2% ARS (pH 4.2) solution similar to conducted in the VSMCs. After staining, the slides were mounted and images were taken with a light microscope (Zeiss, Germany). Calcified areas are shown as red staining.

As to ARS staining for paraffin-embedded tissue, Paraffin-embedded human carotid arteries (5 µm sections) were deparaffinized in xylene and hydrated to 70%

ethanol. After rinsing in ddH<sub>2</sub>O, sections were fixed with 4% PFA for 15 minutes and stained with 0.2% ARS (pH 4.2) solution for 3-5 minutes as described above. After staining, the slides were cleared in xylene and finally mounted. The resultant slides were scanned at 20 × via an Aperio® ScanScope XT slide scanner (Leica Biosystems, Nussloch, Germany).

**Table S1. List of major antibodies used in the study**

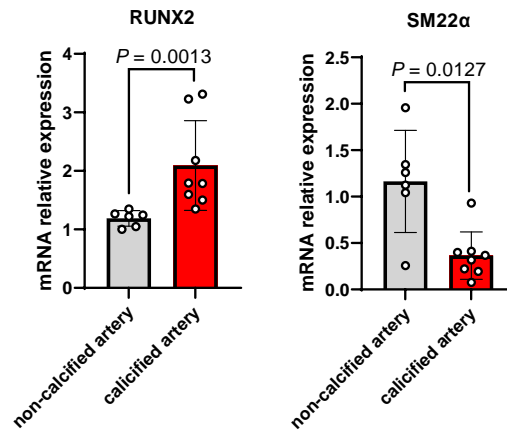
<b>Target antigen</b>	<b>Vendor or Source</b>	<b>Catalog #</b>	<b>Working concentration</b>
human IL-29	Abnova	PAB3666	IHC: 1:200
human IL-29 neutralization antibody	R&D systems	AF1598	Neutralization: 10 µg/ml
human/rat BMP2	Servicebio	GB11252	IHC: 1:400; WB: 1:1000
human IL-10R2	R&D systems	MAB874	IF: 1: 200
human IL-28R $\alpha$	Mybiosource	MBS820358	IF: 1: 200
mice IL-28a	Santa Cruz	sc-137151	IF: 1: 200
mice/rat IL-10R2	Santa Cruz	sc-271969	IF: 1: 200
mice/rat IL-28R $\alpha$	Mybiosource	MBS9130569	IF: 1: 200
IL-28R $\alpha$ neutralization antibody	Mybiosource	MBS822916	Neutralization: 10 µg/ml
mice $\alpha$ -SMA	Abcam	ab5694	IF: 1: 200
RUNX2	Cell Signaling Technology	#12556	WB: 1:1000
GAPDH	Cell Signaling Technology	#2118	WB: 1:1000
p-JAK2	Beyotime	AF1486	WB: 1:1000
JAK2	Beyotime	AF1489	WB: 1:1000
Phosphor-Stat antibody sampler kit	Cell Signaling Technology	#9914	WB: 1:1000

Stat antibody sampler Kit II	Cell Signaling Technology	#93130	WB: 1:1000
Phospho-STAT4 (Tyr693) antibody	Affinity	AF3441	WB: 1:1000
p-p38	Cell Signaling Technology	#9211S	WB: 1:1000
p38	Cell Signaling Technology	#9612	WB: 1:1000
p-ERK	Cell Signaling Technology	#9101S	WB: 1:1000
ERK	Cell Signaling Technology	#4695S	WB: 1:1000
p-JNK	Cell Signaling Technology	#9251S	WB: 1:1000
JNK	Cell Signaling Technology	#9252	WB: 1:1000

**Table S2. Primers used for quantitative real time PCR**

Gene	Forward (5'-3')	Reverse (5'-3')
human IL-29	GAAGCAGTTGCGATTTAGCC	GAAGCTCGCTAGCTCCTGTG
human IL-28R $\alpha$	CCTCCCCAGAATGTGACGC	CCCGCACACTCTTCCACTT
human IL-10R2	TACCACCTCCCGAAAATGTCA	CCCAGTCTGAATGCTCATCTG
human BMP2	ACCCGCTGTCTTCTAGCGT	TTTCAGGCCGAACATGCTGAG
human GAPDH	GGAGCGAGATCCCTCCAAAAT	GGCTGTTGTCATACTTCTCATGG
human RUNX2	TGGTTACTGTTCATGGCGGGTA	TCTCAGATCGTTGAACCTTGCTA
human SM22 $\alpha$	AGTGCAGTCCAAAATCGAGAAG	CTTGCTCAGAATCACGCCAT
rat IL-28R $\alpha$	CCTGGAATACATTTTTGATGTGGAG	TTCAGTTCCAGTGACCGAGG
rat IL-10R2	GCCAGCTCTAGGAATGAT	AATGTTCTTCAAGGTCCAC
rat BMP2	ATTAGCAGGTCTTTGCACCAAGAT	CCCTCCACAACCATGTCCTGA
rat OPN	GGTTTGCTTTTGCCTGTTCG	GTCCTCATCTGTGGCATCGG
rat $\alpha$ -SMA	AACTGGTATTGTGCTGGACTCTG	CTGTTATAGGTGGTTTCGTGGAT
rat SM22 $\alpha$	ATCCAAGCCAGTGAAGGTGC	GACTGTCTGTGAACTCCCTCTTA
rat GAPDH	GGCACAGTCAAGGCTGAGAATG	ATGGTGGTGAAGACGCCAGTA

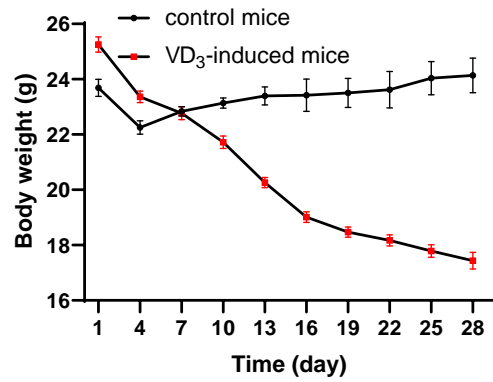
**Figure S1. Runx2 and SM22 $\alpha$  expression are increased in calcified arteries from patients with coronary artery disease (CAD) and chronic kidney disease (CKD)**



Quantitative real time PCR assay (qPCR) showed increased Runx2 and decreased SM22 $\alpha$  mRNA expression in the non-calcified carotid arteries (n = 6) compared with calcified ones (n = 8). Data are mean  $\pm$  SD. Statistical significance was tested using Mann-Whitney U test. RUNX2: Runt-related transcription factor 2; SM22 $\alpha$ : smooth muscle 22 $\alpha$ .



**Figure S2. The changes in body weight are in response to vitamin D<sub>3</sub> treatment in C57BL/6 mice**



Vitamin D<sub>3</sub> treatment in mice (n = 10) resulted in significant body weight loss over the course of the study compared to olive oil vehicle (n = 5). Weights were assessed every three days. Data are mean  $\pm$  SEM.